

RESEARCH PAPER

Aromatic Product Selectivity of Template-Free and Template-Synthesized ZSM-5 Catalysts in Methanol to Hydrocarbon Conversion

Atefeh Saber¹, Maryam Jabbarpoor¹, Nasser Safari^{1*}, Farzad Bahadoran^{2*}

¹ Department of Chemistry, Shahid Beheshti University, Evin, Tehran, Iran

² Gas Research Division, Research Institute of Petroleum Industry (RIPI), Tehran, Iran

ARTICLE INFO

Article History:

Received 14 March 2022

Accepted 17 March 2022

Published 1 May 2022

Keywords:

ZSM-5

Seed-assisted

Template free

MTH

BTX

ABSTRACT

Template-free ZSM-5 zeolites with the SiO₂/Al₂O₃ ratios of 28, 50, and 80 were synthesized and compared with template preparation. The resulting zeolites were characterized by IR, XRD, XRF, SEM, and BET analyses. The template-free and SDA (synthetic directing agent, or with template) zeolites manifested similar physical and chemical characteristics. In addition, their catalytic performances were tested for methanol to hydrocarbon (MTH) as an industrial process in which methanol produced from any source can be converted to a wide range of hydrocarbons (from olefins to gasoline and aromatic hydrocarbons) in a fixed-bed reactor. The zeolites showed methanol conversions of 93.5 and 92.6% for the SiO₂/Al₂O₃ ratio of 50 with the template HZ-50T and template-free HZ-50, respectively. Further, their product selectivity was also similar; nonetheless, eliminating the templates in the preparation of the zeolites had little effect on the conversion and selectivity of the products. The ratio of aromatic to aliphatic decreased with an increase in the SiO₂/Al₂O₃ ratio. Furthermore, raising the SiO₂/Al₂O₃ ratio (from 28 to 80) reduced the gaseous product from 54.1% to 52.1%.

How to cite this article

Saber A., Jabbarpoor M., Safari N., Bahadoran F. Aromatic Product Selectivity of Template-Free and Template-Synthesized ZSM-5 Catalysts in Methanol to Hydrocarbon Conversion. *Nanochem Res*, 2022; 7(2):93-106. DOI: 10.22036/ncr.2022.02.005

INTRODUCTION

ZSM-5 zeolites are a group of aluminosilicate compounds with a pentasil structure [1], having significant applications in agriculture [2], medicine [3], and oil industries [4,5]. It is generally acknowledged that the strong acidity and distinctive porous structure of HZSM-5 zeolite results in its wide use in the methanol to aromatic (MTA) process [6–9]. Due to the increasing demand for BTX (Benzene, Toluene, and Xylenes) in the preceding decades, improving the selectivity toward aromatic products has been the objective of much research [6,10]. Various strategies have been investigated for achieving this goal such as post-treatment, direct synthesis, impregnation,

and many other methods [7,11]. The strong acid sites of ZSM-5 are recognized as their active sites for producing aromatic hydrocarbons and coke. In addition, acidic sites in zeolite are essential for their reactivity, especially in MTH and MTA processes. However, further dehydrogenation of hydrocarbons on the acidic site is one of the mechanisms for coke formation. ZSM-5 with hierarchical canals and an appropriate pore size is a suitable catalyst for aromatic formation; however, coking the catalyst is a challenging issue due to its efficiency. Attempts have been made to adjust the acidic character of the catalysts by altering the SiO₂/Al₂O₃ ratio or by adding metal promoters for preventing coke formation [12]. Many efforts have been undertaken to determine the relationship between the ZSM-5 structure and its performance

* Corresponding Author Email: n-safari@sbu.ac.ir
bahadoranf@ripi.ir

in the MTA process [13]. According to Gao et al. [14], ZSM-5 with $\text{SiO}_2/\text{Al}_2\text{O}_3 = 100$ demonstrated the highest selectivity to BTX due to its adequate acid density and strength. Further, Yang et al. [15] studied the relationship between HZSM-5 crystal size and the synthesis of aromatic hydrocarbons, and they found that nano-sized HZSM-5 exhibited notable selectivity toward aromatics.

Alex Cronsted synthesized zeolites for the first time in 1756 [16]. Since then, a variety of synthetic methods have been proposed, with hydrothermal synthesis being the most popular [17]. Two base materials are usually used as the source for Al and Si to synthesize zeolites [16]. Furthermore, a cation such as Na or K and a synthetic directing agent (SDA) are necessary for the formation of zeolites [18–20]. Although employing a template has drawbacks such as greater costs and bio-environmental contamination, which is required for producing hierarchical zeolites with high crystallinity rates such as ZSM-5 [21]. Therefore, much research has been conducted in the last decades for minimizing organic templates, replacing traditional SDA with cheaper alternatives, recycling templates, and eventually removing SDA by using the seed pattern [19,22–24]. Due to their simple crystal structures, some of zeolites can be synthesized in large quantities using the common synthetic method, without the need for organic templates [25]. However, ZSM-5's hierarchical structure makes the process a bit more challenging [26,27]. Hence, in the absence of templates, using zeolite seeds may be a logical solution to the problem [19]. In order to produce a beta zeolite, Xie and his colleagues (2008) made the first attempt at synthesizing without a template by using seeds [28]. In 2012, Okubo and his team managed to conduct this process for synthesizing ZSM-5 and ZSM-11 zeolites [29,30].

In this study, we tried to synthesize ZSM-5 zeolites in different $\text{SiO}_2/\text{Al}_2\text{O}_3$ ratios without a template and by using zeolite seeds. We successfully synthesized ZSM-5 zeolites with different ratios of $\text{SiO}_2/\text{Al}_2\text{O}_3$ up to 80. However, in the absence of a template, attempts to make the zeolite with higher silicon to aluminum ratios were unsuccessful. Huimi Luan et al. have recently reported the synthesis of high silica ZSM-5 by applying a combined method of seeding and aluminum silicate precursor in which water is replaced with ethanol in the absence of organic templates except alcohol [31]. However, the detail comparison of catalytic efficiency need to

be investigated further. In this work, the template-free zeolites and template-synthesized zeolites were both employed in a fixed-bed reactor to compare their performances in the MTH process.

EXPERIMENTAL METHOD

Material and Methods

All the materials were supplied by chemical companies mentioned below and used as received: tetra propyl ammonium bromide (Merck), silica sol 40 wt% suspensions in water (Sigma), ammonium nitrate NV 98% (Chem-Lab), aluminum sulfate (Merck), industrial ZSM-5 with $\text{SiO}_2/\text{Al}_2\text{O}_3$: 28 (Petroleum Industry Research Institute of Iran), sulfuric acid 98% (Mojallali), activated carbon (Heycarb). BOMEM, MB-Series FTIR was employed for IR spectroscopy characterization, and sample crystallinity was measured from (1). IR crystallinity is calculated using Eq. 1. In this equation, I_{550} and I_{450} represent the absorption intensities of vibration bands with the wave numbers of 550 and 450 cm^{-1} , respectively.

$$IR \text{ Crystallinity} = \frac{I_{550}/I_{450}}{0.72} * 100\% \quad (1)$$

The powders X-ray diffraction were used by STOE X-Ray diffractometer tube anode: Cu, wavelength 1.5406 Å (Filter Ni) with Cu K α radiation (40 kV, 40 mA) over 2θ range between 0° and 80° to identify the crystalline phase. The relative crystallinity and average crystallites size were calculated using Equations 2 and 3, respectively.

$$\text{Crystallinity}(\%) = \frac{I_c}{(I_c + I_D)} * 100 \quad (2)$$

$$D = \frac{K \lambda}{\beta \cos \theta} \quad (3)$$

Where I_c denotes the integrated area of all crystalline peaks; $(I_c + I_D)$ represents the total integrated area under the XRD peaks (I_D = Integrated area of amorphous peaks); D is the crystallites size (nm), $K = 0.9$ (Scherer constant), $\lambda = 0.15406$ (nm) is the wavelength of X-Ray sources, β = FWHM (radians), θ = peak position (radians). The final results are shown in Table 2. The morphology and size of particles were observed by scanning electron microscopy (SEM) (ZEISS, ETH=15.00 KV, WD = 6.5 mm, Mag = 500 x). The pore size, pore volume, and surface areas were determined by the BET method through nitrogen adsorption and desorption (Micromeritics Instrument Corporation, TriStar II 3020 V1.03). The samples

Table 1. Name of the synthesized sample.

Sample	Name
SiO ₂ /Al ₂ O ₃ = 28	HZ-28
SiO ₂ /Al ₂ O ₃ = 50	HZ-50
SiO ₂ /Al ₂ O ₃ = 80	HZ-80
SiO ₂ /Al ₂ O ₃ = 50 with Template	HZ-50T
SiO ₂ /Al ₂ O ₃ = 50 with mesoporgen	HZ-50C

were placed at 30 °C for 10 minutes and then at 300 °C for 120 minutes under a nitrogen atmosphere. Subsequently, nitrogen adsorption and desorption isotherms were obtained at nitrogen boiling temperature (77 K) and a relative pressure range of 0.05-0.99. Each product was measured by XRF (PHILIPS, PW1410) to get its bulk SiO₂/Al₂O₃ ratio to compare it with the ratio of starting gel (Table 2).

Synthesis of H-ZSM-5

Template free synthesis of H-ZSM-5

H-ZSM-5 zeolites with SiO₂/Al₂O₃ ratios of 28, 50, and 80 were synthesized by the hydrothermal method. Solution A was obtained by adding 51.6 g water glass (a suspension of 40% by weight of silica sol in water), to 64.5 g deionized water and 0.5 g seed, and the mixture was stirred for 10 min. Solution B was prepared by mixing X g of Al₂(SO₄)₃·18 H₂O with 4.2 g concentrated sulfuric acid in 84.1 g water and stirring for 30 min (X= 5.4 g, 3.0 g, 1.9 g, respectively). Solution B was added dropwise to solution A and stirred at room temperature at 300 rpm for 1 hour. The molar composition of the mixture was 1.35 Na₂O: 50 SiO₂: X Al₂O₃: 2199 H₂O where X was 1, 1.78, and 0.625: Seed to SiO₂ mass

ratio was 5%. The resulting gel was transferred to a Teflon lined autoclave and remained there at 180 °C for 48 hrs for hydrothermal treatment. The resulting crystals were filtered off, washed with deionized water three times, and dried at 110 °C overnight. The ion exchange with 1M ammonium nitrate was performed twice and filtered. Finally, the filtrate was calcined at 550 for 5 hrs to obtain H-ZSM-5.

Synthesis of H-ZSM-5 zeolites with Mesoporgen or Template

For preparing the zeolite in the presence of mesoporgen (carbon active), the same procedure as before was followed; however, when the gel was formed, 0.5 g of carbon active was added to it. The gel composition was: 1.35 Na₂O: 50 SiO₂: Al₂O₃: 2199 H₂O and the carbon active to SiO₂ mass ratio was 5%. For template synthesis of the zeolite, tetra propyl ammonium bromide was added to the Si source with the mole ratio of 1.35 Na₂O: 50 SiO₂: 1Al₂O₃: 2199 H₂O: 4.5 TPABr. Prior to the ammonium ion exchange, the products were calcined at 550 °C for 5 hrs. The prepared H-ZSM-5 samples were named in Table 1.

Table 2. The relative crystallinity & crystal size of zeolites (Chemical composition of the starting materials for the synthesis of zeolites determined by XRF).

Sample	Relative Crystallinity (XRD)	Relative Crystallinity (IR)	Crystal size (nm)	SiO ₂ /Al ₂ O ₃ Product (XRF)
HZ-28	67.5%	69.9%	27.5	26.7
HZ-50	83.8%	78.4%	28.9	47
HZ-80	67%	68.7%	18.4	70.6
HZ-50C	77.6%	72.1%	27.9	-
HZ-50T	100%	87.85%	28.6	-



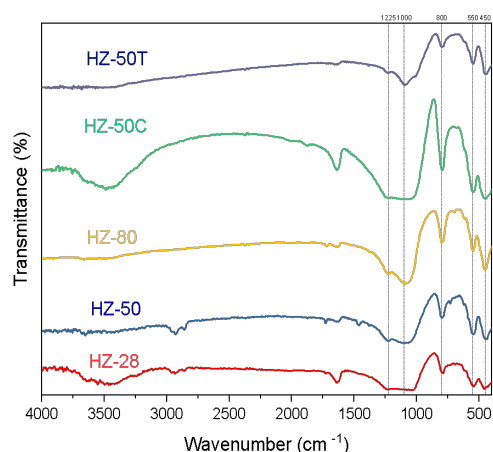


Fig. 1. FTIR spectra of the different ZSM-5 zeolites.

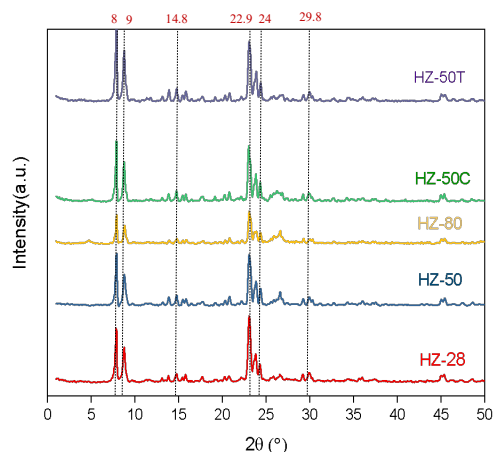


Fig. 2. XRD patterns of the different ZSM-5 zeolites.

RESULTS AND DISCUSSION

The XRD and FTIR patterns

Fig. 1 illustrates the FT-IR spectrum of the prepared samples in the range of 400–4000 cm^{-1} . The formation of the MFI framework of H-ZSM-5 was confirmed by 450, 550, 1100 and 1200 cm^{-1} bands. The IR of the samples prepared with the seeds, the template, and the mesoporgen matched with the reported ZSM-5 [20]. In the absence of the template, many attempts were made to prepare H-ZSM-5 with a $\text{SiO}_2/\text{Al}_2\text{O}_3$ ratio of higher than 100; nonetheless, they failed to produce a pure zeolite. It seems that a template is required for the synthesis of the ZSM-5 with a high $\text{SiO}_2/\text{Al}_2\text{O}_3$ ratio. The X-ray diffraction pattern for the ZSM-5 zeolite structure in Fig. 2 exhibits all the feature picks at $2\theta = 8.0^\circ, 9.0^\circ, 14.8^\circ, 22.9^\circ, 24.0^\circ, 29.8^\circ$ as expected [32]. In addition, XRD confirmed the successful synthesis of template-free ZSM-5 samples with $\text{SiO}_2/\text{Al}_2\text{O}_3$ ratio below 80 [33]. The structure, purity, and high crystallinity of the synthesized samples were demonstrated by XRD and FTIR spectroscopy, and by comparing with the HZ-50T sample. In general, the XRD patterns of carbon-template zeolites, HZ-50C, are of lower intensity than conventional ZSM-5 (without carbon), which could be accounted for in terms of a lower density of mesoporous in ZSM-5 zeolite crystals [33].

Table 2 indicates the relative crystallinity and crystal sizes of ZSM-5 compared to that of the HZ-50T sample by IR and XRD measurements. Increasing the $\text{SiO}_2/\text{Al}_2\text{O}_3$ ratio from 28 to 50 resulted in increasing the crystallinity and crystal size of the samples. However, by raising the $\text{SiO}_2/\text{Al}_2\text{O}_3$ ratio from 50 to 80, the crystallinity of the samples and the size of the crystals decreased. With

a higher $\text{SiO}_2/\text{Al}_2\text{O}_3$ ratio, zeolites could not be purely prepared. HZ-50T prepared in the presence of a template demonstrated a slightly better crystallinity. It has been noted in some articles that when the $\text{SiO}_2/\text{Al}_2\text{O}_3$ ratio rises, the crystallinity of zeolites ZSM-5 increases [34]. This may be true for zeolites prepared in the presence of a structure-directing agent; however, in the samples prepared in this study, the maximum crystallinity was observed in the ratio of 50.

According to Table 2 (rows 1–3), the crystal size of ZSM-5 gradually increases with increasing the $\text{SiO}_2/\text{Al}_2\text{O}_3$ molar ratio in its synthetic gel. Although the crystal size is estimated by Scherer's approximation and should be considered with caution, it is directly related to crystallinity. The sample with lower crystallinity shows a smaller crystal size, resulting from weaker diffraction peaks [35]. Based on the results obtained from the XRF analysis in Table 2, the $\text{SiO}_2/\text{Al}_2\text{O}_3$ ratio of the final samples is lower than that of the initial gel. The gap between $\text{SiO}_2/\text{Al}_2\text{O}_3$ ratios increased by raising $\text{SiO}_2/\text{Al}_2\text{O}_3$ ratio. This difference was not unexpected considering the issues with the synthesis of non-template zeolites. As the $\text{SiO}_2/\text{Al}_2\text{O}_3$ ratio increases, the entrance of Al atoms in the zeolite structure becomes more difficult.

NH_3 -TPD

The type, density, and distribution of acidic sites on the investigated catalyst is one of the most significant and determining parameters on the performance of catalysts in the MTH process, and this can be studied by using the NH_3 -TPD analysis.

The acid sites on the surface of ZSM-5 samples mainly consist of three types: weak (100–220 $^\circ\text{C}$),

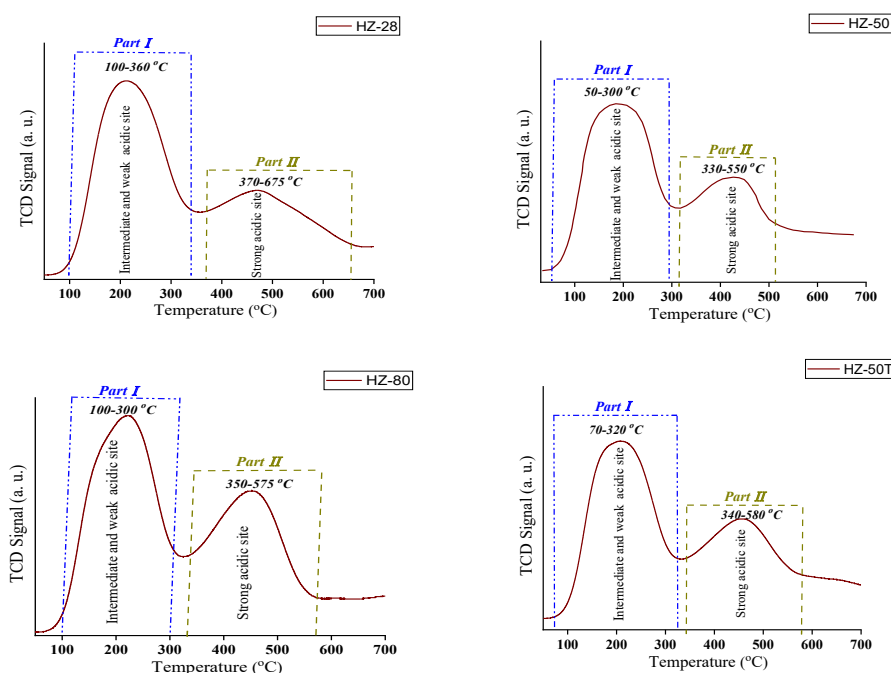


Fig. 3. NH_3 -TPD profiles of the hierarchical HZSM-5 zeolites with different Si/Al ratios.

medium (220–390 °C), and strong (390–600 °C). However, due to their overlap, only two of these types appear as peaks in the NH_3 -TPD test.

As shown in Fig. 3 and Table 3, the amount of the total, weak, and strong acidities in HZ-50 and HZ-50T are close to each other, showing the similarity of the template and seed samples. Moreover, it can be observed that the total acidity reduces as $\text{SiO}_2/\text{Al}_2\text{O}_3$ ratio increases (HZ-28 > HZ-50 > HZ-80). This reduction indicates, as predicated, that by increasing the amount of Al in the structure, more acidic sites are produced [14,36]. These findings may be consistent with those obtained from the catalytic performance of samples in the MTH process. Based on the NH_3 -TPD results, Fig. 6 demonstrates similarity in the conversion, liquid, and gas products for HZ-50 and HZ-50T, which can be attributed to their similar acidity.

The more acidity the catalyst has, the more

aromatic compounds can be produced; however, the catalyst's higher acidity leads the formation of more coke. Therefore, a catalyst with high acidity should be used to produce more aromatic compounds, however coke formation should also be considered [14,37]. According to NH_3 -TPD, HZ-50 has high acidity, although it's not as high as HZ-28, which can yield more aromatic products with a lower likelihood of coke formation.

SEM

The SEM images show the size, morphology, and aggregation of the synthesized zeolites. As shown in Fig. 4, the morphology of the zeolites obtained with various initial $\text{SiO}_2/\text{Al}_2\text{O}_3$ ratios or by mesoporegen in the absence of SDA was almost identical; these particles have hexagon plate-like features. Furthermore, Fig. 4 demonstrates that they have similar particle sizes while the HZ-50

Table 3. NH_3 -TPD data and acid amount for the hierarchical HZSM-5 zeolites with different Si/Al ratios.

Sample	Acid amount (mmol g^{-1})		
	Total acidity	Weak acidity	Strong acidity
HZ-28	1.56	0.92	0.64
HZ-50	1.03	0.61	0.42
HZ-80	0.94	0.54	0.4
HZ-50T	1.16	0.69	0.47



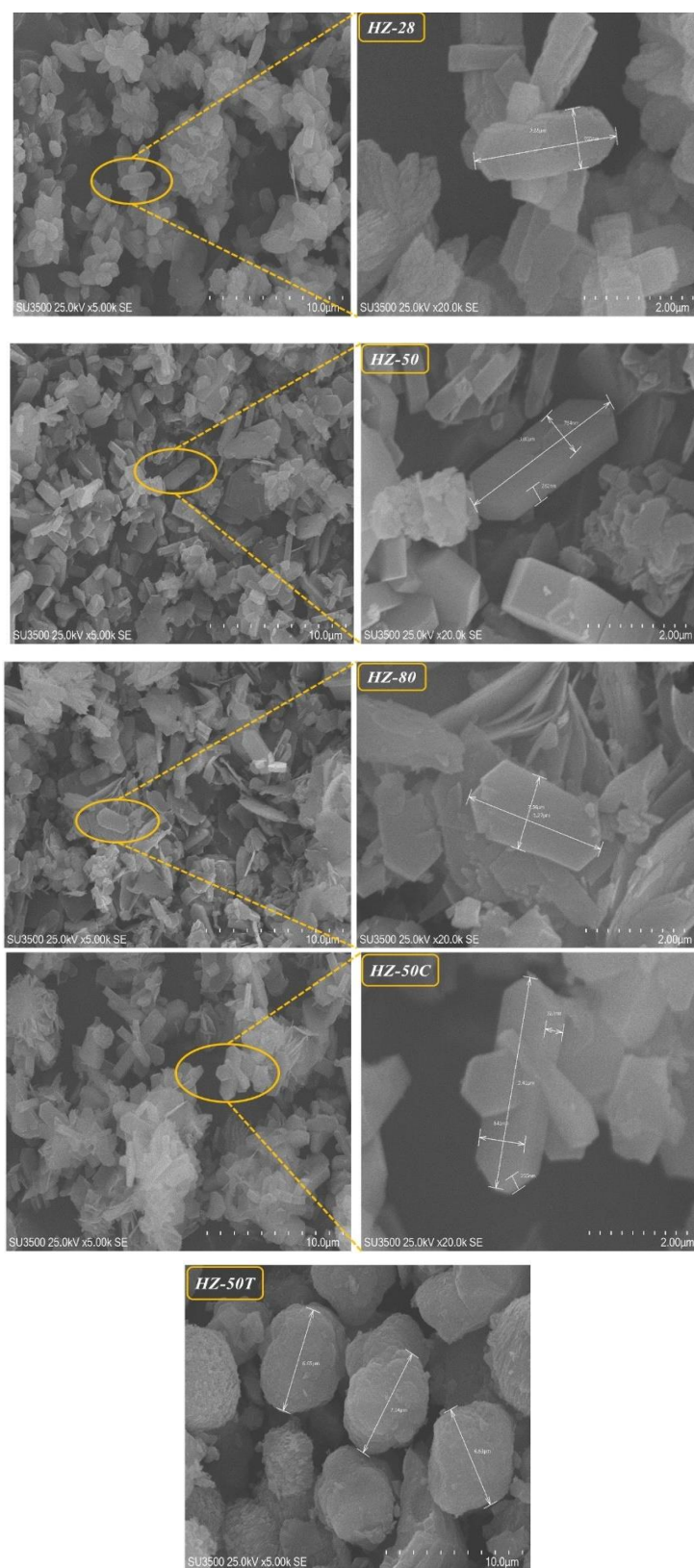


Fig. 4. SEM image of the samples after crystallization and calcination.



sample has a better crystalline shape in accordance with the IR and XRD data. However, in addition to having a spherical morphology, the HZ-50T zeolite synthesized by using the templates has a larger particle size which may indicate the agglomeration of particles. Nonetheless, the XRD confirms that the crystal size of the samples with both template and template-free zeolites is almost the same (around 20-30 nm).

BET and pore size distribution analysis

In the BET analysis, the surface area of the samples was measured, and the volume of the micro and mesopores was calculated by using the T-plot method. The adsorption and desorption isotherms for zeolites are type I [38] (Fig. 5), indicating the

mesoporosity alongside the micropore structure. The pore size distributions measured by the BJH method of various ZSM-5 samples are shown in Table 4. As the results in Table 4 indicate, the surface area (S_{BET}) of the samples with different ratios is almost equal and similar to that of the sample synthesized in the presence of the structure-directing agent. However, in the $\text{SiO}_2/\text{Al}_2\text{O}_3$ ratio of 80, the mesoporosity of the zeolite considerably reduced. The decrease in surface area in the HZ-50C sample can be justified by its increased mesoporosity, since increasing the volume of the mesopores will reduce the surface area in most cases. The activated carbon was employed to produce a mesoporous structure. The mesoporous structure of the HZ-50C was confirmed by the formation of

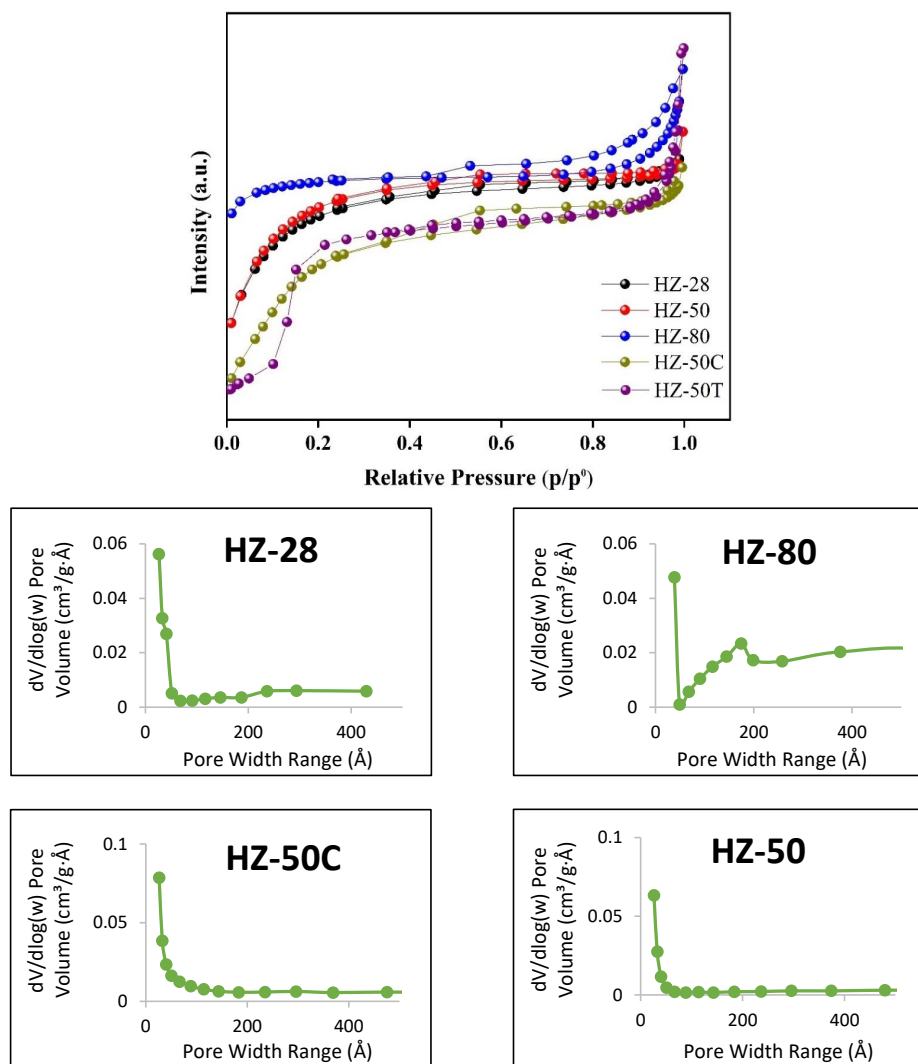


Fig. 5. The N_2 adsorption and desorption isotherms of zeolites & BJH by the BET method.



Table 4. The textural properties of different samples.

Sample	surface area (m^2/g)			Pore volume (cm^3/g)			Crystal Size (nm)	Average Pore Size (nm)
	S_{BET}	S_{Micro}	S^I_{Meso}	V_{Total}	V_{Micro}	V^2_{Meso}		
HZ-28	360.85	274.62	86.23	0.176	0.126	0.049	16.62	1.95
HZ-50	365.03	272.42	92.61	0.175	0.125	0.049	16.43	1.92
HZ-80	369.90	352.17	17.73	0.187	0.164	0.023	16.22	2.02
HZ-50C	340.94	212.03	128.9	0.170	0.097	0.073	17.59	2.00
HZ-50T	361.04	305.42	55.62	0.192	0.160	0.032	16.20	2.13

¹ t-Plot External Surface Area² $V_{meso} = V_{ads} - V_{micro}$

the hysteresis lobe at relatively high pressures. In addition, the structure-directing agent in HZ-50T led to a higher mesoporosity, which could be an advantage for this sample; nevertheless, it also has economic and environmental disadvantages.

CATALYTIC MTH ACTIVITY

The template-free zeolites and SDA samples have very similar physical natures; therefore, they are suitable for comparing their applicability. The function of the synthesized zeolites was checked by the MTH process. The calcined catalysts were loaded in a steel fixed-bed reactor, and the catalytic performances were tested at atmospheric pressure in WHSV $3h^{-1}$ and temperature of $400^\circ C$. Crossing gases were monitored by mass flow controllers. The liquid products were collected in a cold trap, while the gaseous products were guided to an on-line gas chromatograph during the reaction. After collecting the liquid product and separating the aqueous and organic phases, the organic liquid product was also analyzed using a DHA analysis by Varian 3800 gas chromatograph.

Table 5 shows product selectivity obtained with various HZSM-5 catalysts at $400^\circ C$ and atmospheric pressure. The conversion percent of the methanol, gas, and liquid products are summarized in Fig. 6. Based on Table 5 and Fig. 6, the HZ-50T sample has the highest methanol conversion rate among other samples, which can be related to its higher crystallinity (100%). It may be concluded from comparing two synthetic samples with an equal SiO_2/Al_2O_3 ratio (HZ-50, HZ-50T) that the absence of a template had little effect on the conversion of the reaction. This could be a sign of functional similarity between the two catalysts.

Moreover, HZ-50T has the highest selectivity of liquid products, and HZ-50C gave the highest yields for gaseous products, probably due to the channel structure of mesoporous ZSM-5 crystals [39]. In addition, a decrease in the external surface area and an increase in the mesopores could enhance short-chain hydrocarbons (gaseous product) as in HZ-50C [39] (Table 5).

An important effect of increasing Si/Al ratio was a decrease in the gaseous product, from 54.1%

Table 5. Conversion percent and selectivity of the products based on the number of carbons in MTH process at P = 1atm, T = $400^\circ C$, WHSV = $3h^{-1}$.

Sample	MeOH Conv.% (± 0.2)	Selectivity, mol% (± 0.2)									
		C ₁	C ₂	C ₃	C ₄	C _{1-C₄}	C ₅	C ₆	C ₇	C ₈	C ₉₊
HZ-28	91.4	5.4	5.5	40.8	7.5	59.2	6.7	1.7	10.9	13.6	7.9
HZ-50	92.6	5.7	5.4	37.5	7.7	56.1	9.1	1.3	10.3	14.8	8.3
HZ-80	90.7	6.5	4.6	35.6	10.4	57.1	10.7	0.9	8.7	14.4	8.2
HZ-50C	88.6	4.3	14.2	27.1	14.1	59.7	11.1	0.8	8.6	11.7	8.1
HZ-50T	93.5	3.1	6.3	36.9	9.4	55.7	8.6	1.8	14.3	11.3	8.3

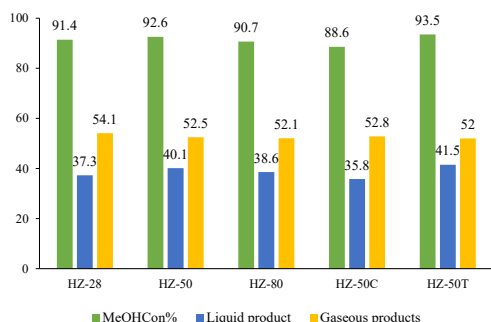


Fig. 6. Methanol conversion, liquid product, and gaseous product in HZ-28, HZ-50, HZ-80, HZ-50C, HZ-50T samples for $P = 1 \text{ atm}$, $T = 400 \text{ }^\circ\text{C}$, $\text{WHSV} = 3 \text{ h}^{-1}$.

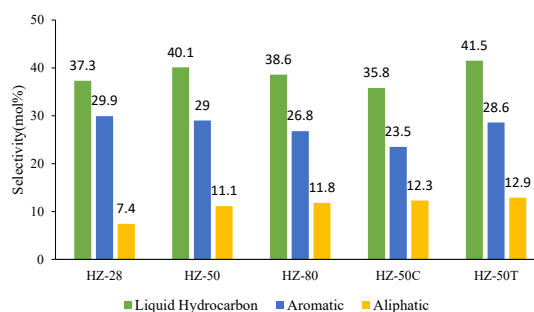


Fig. 7. Liquid hydrocarbon as aromatic and aliphatic in HZ-28, HZ-50, HZ-80, HZ-50C, HZ-50T samples for $P = 1 \text{ atm}$, $T = 400 \text{ }^\circ\text{C}$, $\text{WHSV} = 3 \text{ h}^{-1}$.

to 52.1%, as $\text{SiO}_2/\text{Al}_2\text{O}_3$ ratio increased from 28 to 80 (Fig. 6). Further, the ratio of aromatic to aliphatic liquid product decreases with an increase in the $\text{SiO}_2/\text{Al}_2\text{O}_3$ ratio. Based on Fig. 7, the lowest aromatic to aliphatic ratio belongs to the HZ-50C catalyst (1.9). By comparing the HZ-50T and HZ-50 catalysts, it can be observed that the amount of aliphatic product is more in the template-synthesized catalyst. (HZ-50= 2.6, HZ-50T= 2.2)

The selectivity of the liquid hydrocarbon products is almost identical in various $\text{SiO}_2/\text{Al}_2\text{O}_3$ ratio catalysts (HZ-28, HZ-50, HZ-80) with a slight difference in the HZ-50 catalyst, which can be attributed to better structural properties like crystallinity. As illustrated in Fig. 7, the main products in liquid hydrocarbons are aromatics; however, their selectivity is obviously dependent on the $\text{SiO}_2/\text{Al}_2\text{O}_3$ ratio. To begin with, the liquid hydrocarbon distribution increased with the $\text{SiO}_2/\text{Al}_2\text{O}_3$ molar ratio, which was then followed by a

gradual decline. The highest selectivity of liquid products is related to HZ-50T with 41.5%. More acidic sites in the low $\text{SiO}_2/\text{Al}_2\text{O}_3$ ratio lead to the formation of more aromatics products in HZ-28. The ratio of aromatic to aliphatic yields is around 4 in HZ-28 and reduces to 2.6 and 2.3 in HZ-50 and HZ-80, respectively. The lowest aromatic to aliphatic ratio is seen in the sample prepared in the presence of mesopore, HZ-50C=1.9.

As shown in Fig. 8, the highest percentages of liquid products are xylene and toluene. As the BTX selectivity fell, the $\text{SiO}_2/\text{Al}_2\text{O}_3$ ratio decreased. The higher BTX value obtained for HZ-28 may be due to a higher acidic density in the low $\text{SiO}_2/\text{Al}_2\text{O}_3$ ratio. Comparing the selectivity of BTX between HZ-50T with other catalysts, it can be said that this catalyst behavior for BTX formation is different from other catalysts, in which the lowest amount of BTX formation ensues. In addition, all the samples produce more xylene than toluene, while in the

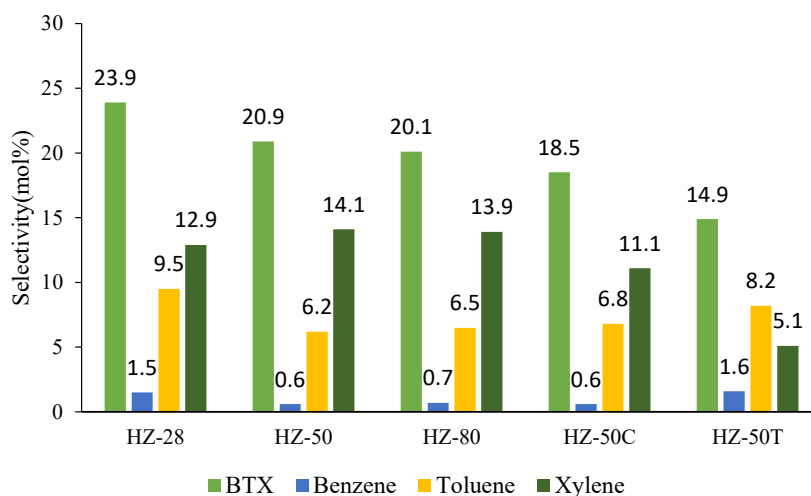


Fig. 8. Selectivity of BTX products in HZ-28, HZ-50, HZ-80, HZ-50C, HZ-50T samples for $P = 1 \text{ atm}$, $T = 400 \text{ }^\circ\text{C}$, $\text{WHSV} = 3 \text{ h}^{-1}$.



Table 6. Weight selectivity of hydrocarbon compounds in the liquid product of HZ-28, HZ-50, HZ-80, HZ-50C, HZ-50T catalysts in P = 1atm, T = 400°C, WHSV = 3 h⁻¹.

Sample	Selectivity (WT%)				
	Aromatic	Iso-Paraffins	Naphthenes	Olefins	Paraffins
HZ-28	93.87	4.5	0.29	1.01	0.28
HZ-50	93.97	2.23	0.81	2.09	0.91
HZ-80	94.1	3.21	1.34	1.01	0.35
HZ-50C	89.94	3.13	1.97	3.3	1.67
HZ-50T	91.66	5.67	0.57	1.75	0.36

case of the HZ-50T, which is the sample prepared in the presence of a template, the main product is toluene. This difference in selectivity may be related to different hierarchical structures produced by the template and template-free route.

The yields for gaseous products C₁-C₄ increased in the order of HZ-50C > HZ-28 > HZ-50 > HZ-80 > HZ-50T (Fig. 9). The main product in the gaseous mixture is propene. The yield of C₃ compounds decreased considerably in HZ-50C at the expense of C₂ and C₄. Hence, it seems that these catalysts are highly effective for C₃⁺ and aromatic production processes. By increasing the amount of SiO₂/Al₂O₃, gaseous to liquid products slightly decreased.

During this stage, the selectivity of liquid products was also studied in order to compare our results with previous works (Tables 7 and 8). Based on Fig. 10 and Table 6, the aromatic compounds are the major products in the liquid phase. The highest amounts of aromatics compounds belong to the HZ-80 catalyst, which demonstrates that this catalyst can be a suitable candidate for the MTA process.

Several studies were conducted on the MTH process in the literature, and some of the summarized results can be seen in Tables 7 and

8. It should be noted that the procedure for the synthesis of H-ZSM-5 or the conditions used for reactor analysis may be slightly different. Tables 7 and 8 indicate the fact that the utilized catalysts can have different results based on synthesizing conditions, SiO₂/Al₂O₃ ratio, and the reactor design and condition. For example, Saxena [40] and his colleagues synthesized H-ZSM-5 zeolite using sodium silicate and aluminum nitrate as the synthesis source and TPAOH as the template, with a SiO₂/Al₂O₃ ratio of 50. They have reported yields of 50.7 percent for fuel at T= 400 °C and P=1 atm. Zhao et al. [41] used ZSM-5 zeolites prepared by seed in the presence of a secondary CTAB template as a mesopore maker, and they reported a yield of 59.1 for SiO₂/Al₂O₃=50. Wan and coworkers [42] employed nano size ZSM-5 zeolites using TPABr as a template, and reported 58.9 yields in the MTG process in 10 atm. Overall, it can be observed that a template-free synthesized ZSM-5 catalyst produces a slightly lower yield of gasoline cut compared to that of a template synthesized.

However, based on Table 8, the data reported in this work, and comparing studies on the MTA process, it can be stated that these template-free catalysts seem to be more successful in producing

Table 7. Comparison results with other literature in MTG.

Gasoline Selectivity(mole%)	p	WHSV(h ⁻¹)	SiO ₂ /Al ₂ O ₃	Template	Catalyst	Year	Ref
50.7	1atm	4	50	TPAOH	ZSM-5	2014	[40]
59.1	1atm	16	50	ZSM-5 Seed/CTAB	ZSM-5	2019	[41]
58.9	10atm	1.2	50	TPABr	ZSM-5	2014	[42]
43.9/44.3	1atm	3	50	ZSM-5 Seed or TPABr	ZSM-5	2021	This work

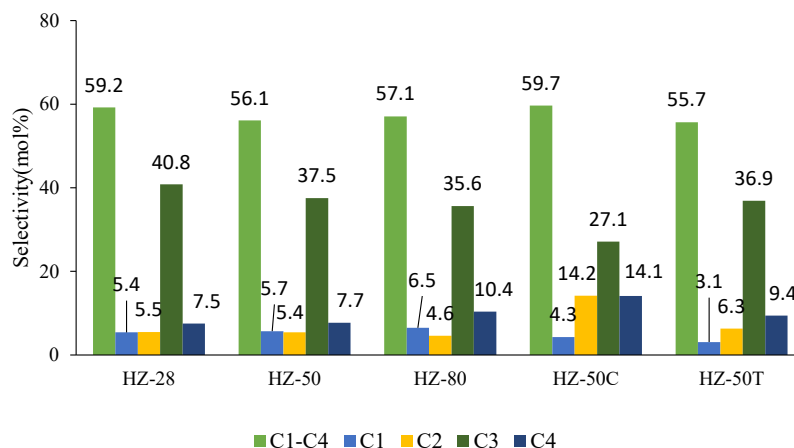


Fig. 9. Gaseous hydrocarbon as carbon number in HZ-28, HZ-50, HZ-80, HZ-50C, HZ-50T samples for $P = 1\text{ atm}$, $T = 400^\circ\text{C}$, $\text{WHSV} = 3\text{ h}^{-1}$.

aromatics. Qiao group [44] reported 85 percent BTX in aromatic products by combining HZSM-5 with unique species of Zn and P. Furthermore, Ghanbari and coworkers [43] studied methanol conversion to aromatic hydrocarbons on a new family of low silicon mesopore catalyst ($\text{SiO}_2/\text{Al}_2\text{O}_3 = 22$) in a fixed bed tabular reactor under atmospheric pressure and a temperature of 375°C and $\text{WHSV} = 2\text{ h}^{-1}$. The catalyst reformed with iron and zinc, and under the influence of an alkaline solution had the most selectivity rate to aromatic products, namely BTX.

Yan and his colleges [14] synthesized ZSM-5 with a $\text{SiO}_2/\text{Al}_2\text{O}_3$ ratio of 60 to 160 using seed formation and organosilicon. They realized that the $\text{SiO}_2/\text{Al}_2\text{O}_3$ ratio plays a major role in morphology structure and acidity of ZSM-5 zeolite as well

as the catalyst life span and coke formation in MTA reaction. On the other hand, high density and strong acidity results in a higher selectivity toward aromatic compounds. The ZSM-5 zeolite with a $\text{SiO}_2/\text{Al}_2\text{O}_3$ ratio of 100 showed the highest selectivity toward BTX. The sample with a lower ratio of $\text{SiO}_2/\text{Al}_2\text{O}_3$ manifested a greater catalyst life span due to its lower acid density and great resistance to carbon sintering. Additionally, there was a co-relation observed between $\text{SiO}_2/\text{Al}_2\text{O}_3$ ratio and coke content.

CONCLUSION

Compared to template synthetic zeolites, zeolites synthesized by the seed-assisted method without using a template only produced up to a $\text{SiO}_2/\text{Al}_2\text{O}_3$ ratio of 80. It can be concluded that

Hydrocarbon Totals by Group Type

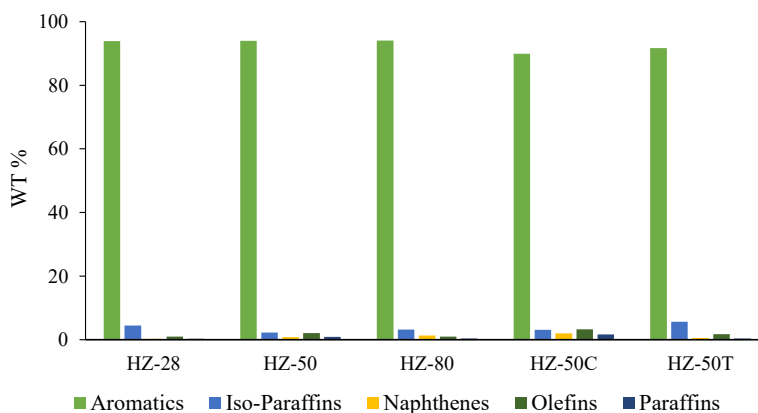


Fig. 10. Weight selectivity of hydrocarbon compounds in the liquid product of HZ-28, HZ-50, HZ-80, HZ-50C, HZ-50T catalysts in $P = 1\text{ atm}$, $T = 400^\circ\text{C}$, $\text{WHSV} = 3\text{ h}^{-1}$.



Table 8. Comparison results with other literature in MTA.

Aromatic Yield(wt%)	P	WHSV(h^{-1})	SiO ₂ /Al ₂ O ₃	Template	Catalyst	Year	Ref
86	1atm	2	50	TPABr	ZSM-5	2018	[43]
61.7	1atm	2	22	TPABr	ZSM-5	2020	[44]
84.6	1atm	10	100	ZSM-5 Seed/ TPAOH organosilicon	ZSM-5	2016	[14]
94.1	1atm	3	50	ZSM-5 Seed	ZSM-5	2021	This Work

SiO₂/Al₂O₃ ratio impacts the properties of the ZSM-5 catalyst as well as the synthesis conditions. In the seed-assisted method without SDA, small cations such as Na⁺ & Al³⁺ were superseded to retain the charge balance of the system. In general, there is not much of a difference in the methanol conversion and selectivity of the products using catalysts synthesized by seed-assisted method or catalysts synthesized with a template. In other words, without a template, the same results can be obtained from the synthetic zeolite.

ACKNOWLEDGMENTS

The authors are grateful to the Research Council of Shahid Beheshti University and Research Institute of Petroleum Industry for supporting this study.

CONFLICT OF INTEREST

The authors declare no conflict of interest.

REFERENCES

- [1] V. Verdoliva, M. S. DeLuca. Zeolites as acid/basic solid catalysts: Recent synthetic developments. *Catalysts*. 2019; 9(3). <https://doi.org/10.3390/catal9030248>
- [2] Ramesh K, Reddy DD. Chapter Four - Zeolites and Their Potential Uses in Agriculture. In: Sparks DL, editor. *Advances in Agronomy*. 113: Academic Press; 2011. p. 219-41. <https://doi.org/10.1016/B978-0-12-386473-4.00004-X>
- [3] Jesudoss S, Vijaya JJ, Kaviyarasu K, Kennedy LJ, Ramalingam RJ, Al-Lohedan HA. Anti-cancer activity of hierarchical ZSM-5 zeolites synthesized from rice-based waste materials. *RSC advances*. 2018;8(1):481-90. <https://doi.org/10.1039/C7RA11763A>
- [4] Jens W. Zeolites and catalysis. *Solid State Ionics*. 2000;131(1-2):175-88. [https://doi.org/10.1016/S0167-2738\(00\)00632-9](https://doi.org/10.1016/S0167-2738(00)00632-9)
- [5] Holderich W, Hesse M, N. umann F. Zeolites: Catalysts for Organic Syntheses. *Angewandte Chemie International Edition in English*. 1988;27(2):226-46. <https://doi.org/10.1002/anie.198802261>
- [6] Wei Z, Xia T, Liu M, Cao Q, Xu Y, Zhu K, et al. Alkaline modification of ZSM-5 catalysts for methanol aromatization: The effect of the alkaline concentration. *Frontiers of Chemical Science and Engineering*. 2015;9(4):450-60. <https://doi.org/10.1007/s11705-015-1542-2>
- [7] Tian H, Yang X, Tian H, Zha F, Guo X, Tang X. Realization of rapid synthesis of H-ZSM-5 zeolite by seed-assisted method for aromatization reactions of methanol or methane. *Canadian Journal of Chemistry*. 2021;99(11):874-80. <https://doi.org/10.1139/cjc-2021-0095>
- [8] Losch P, Boltz M, Louis B, Chavan S, Olsbye U. Catalyst optimization for enhanced propylene formation in the methanol-to-olefins reaction. *Comptes Rendus Chimie*. 2015;18(3):330-5. <https://doi.org/10.1016/j.crci.2014.06.007>
- [9] Missengue RNM, Losch P, Sedres G, Musyoka NM, Fatoba OO, Louis B, et al. Transformation of South African coal fly ash into ZSM-5 zeolite and its application as an MTO catalyst. *Comptes Rendus Chimie*. 2017;20(1):78-86. <https://doi.org/10.1016/j.crci.2016.04.012>
- [10] Zhou F, Gao Y, Ma H, Wu G, Liu C. Catalytic aromatization of methanol over post-treated ZSM-5 zeolites in the terms of pore structure and acid sites properties. *Molecular Catalysis*. 2017;438:37-46. <https://doi.org/10.1016/j.mcat.2017.05.018>
- [11] Ji K, Xun J, Liu P, Song Q, Gao J, Zhang K, et al. The study of methanol aromatization on transition metal modified ZSM-5 catalyst. *Chinese Journal of Chemical Engineering*. 2018;26(9):1949-53. <https://doi.org/10.1016/j.cjche.2018.03.024>
- [12] A.K. Dawagreh, The Role of Catalytic Applications of ZSM-5 Zeolite for Chemical Reaction Processes, (2018).
- [13] Svelle S, Visur M, Olsbye U, Saepurahman, Bjorgen M. Mechanistic Aspects of the Zeolite Catalyzed Methylation of Alkenes and Aromatics with Methanol: A Review. *Topics in Catalysis*. 2011;54(13):897. <https://doi.org/10.1007/s11244-011-9697-7>
- [14] Gao Y, Zheng B, Wu G, Ma F, Liu C. Effect of the Si/Al ratio on the performance of hierarchical ZSM-5 zeolites for methanol aromatization. *RSC Advances*. 2016;6(87):83581-8. <https://doi.org/10.1039/C6RA17084F>
- [15] Yang L, Liu Z, Liu Z, Peng W, Liu Y, Liu C. Correlation between H-ZSM-5 crystal size and catalytic performance in the methanol-to-aromatics reaction. *Chinese Journal of Catalysis*. 2017;38(4):683-90. [https://doi.org/10.1016/S1872-2067\(17\)62791-8](https://doi.org/10.1016/S1872-2067(17)62791-8)
- [16] K.G. Strohmaier. Chapter 3. Synthesis of Zeolites, in: *Zeolites, ExxonMobil Research and Engineering Company, Corporate Strategic Research, 1545 Route 22 East, Annandale, NJ 08801, USA 2017. 73-102 p.* <https://doi.org/10.1039/9781788010610-00073>

- [17] Cundy CS, Cox PA. The Hydrothermal Synthesis of Zeolites: History and Development from the Earliest Days to the Present Time. *Chemical Reviews*. 2003;103(3):663-702. <https://doi.org/10.1021/cr020060i>
- [18] Meng L. Hierarchical MFI zeolites: novel synthesis strategies and applications in catalysis: PhD Thesis, Technische Universiteit Eindhoven (NL); 2018.
- [19] Nada MH, Larsen SC. Insight into seed-assisted template free synthesis of ZSM-5 zeolites. *Microporous and Mesoporous Materials*. 2017;239:444-52. <https://doi.org/10.1016/j.micromeso.2016.10.040>
- [20] Sang S, Chang F, Liu Z, He C, He Y, Xu L. Difference of ZSM-5 zeolites synthesized with various templates. *Catalysis Today*. 2004;93-95:729-34. <https://doi.org/10.1016/j.cattod.2004.06.091>
- [21] Ren N, Bronić J, Subotić B, Lv X-C, Yang Z-J, Tang Y. Controllable and SDA-free synthesis of sub-micrometer sized zeolite ZSM-5. Part 1: Influence of alkalinity on the structural, particulate and chemical properties of the products. *Microporous and Mesoporous Materials*. 2011;139(1):197-206. <https://doi.org/10.1016/j.micromeso.2010.10.043>
- [22] Wang Y, Wu Q, Meng X, Xiao F. Insights into the organotemplate-free synthesis of zeolite catalysts. *Engineering*. 2017; 3: 567-574. doi: 10.1016. *Engineering*. 2017;29. <https://doi.org/10.1016/j.eng.2017.03.029>
- [23] Meng F, Wang Y, Wang S, Wang X, Wang S. Synthesis of ZSM-5 aggregates by a seed-induced method and catalytic performance in methanol-to-gasoline conversion. *Comptes Rendus Chimie*. 2017;20(4):385-94. <https://doi.org/10.1016/j.crci.2016.07.005>
- [24] Wang X, Meng F, Chen H, Gao F, Wang Y, Han X, et al. Synthesis of a hierarchical ZSM-11/5 composite zeolite of high SiO₂/Al₂O₃ ratio and catalytic performance in the methanol-to-olefins reaction. *Comptes Rendus Chimie*. 2017;20(11):1083-92. <https://doi.org/10.1016/j.crci.2017.10.004>
- [25] Travkina O, Agliullin M, Filippova N, Khazipova A, Danilova I, Grigor'Eva N, et al. Template-free synthesis of high degree crystallinity zeolite Y with micro-meso-macroporous structure. *RSC advances*. 2017;7(52):32581-90. <https://doi.org/10.1039/C7RA04742H>
- [26] Yue Y, Gu L, Zhou Y, Liu H, Yuan P, Zhu H, et al. Template-Free Synthesis and Catalytic Applications of Microporous and Hierarchical ZSM-5 Zeolites from Natural Aluminosilicate Minerals. *Industrial & Engineering Chemistry Research*. 2017;56(36):10069-77. <https://doi.org/10.1021/acs.iecr.7b02531>
- [27] Kalipcilar H, Culfaz A. Template-free synthesis of ZSM-5 type zeolite layers on porous alumina disks. *Turkish Journal of Chemistry*. 2007;31(2):233-42.
- [28] B. Xie JS, L. Ren, Y. Ji, J. Li, F.S. Xiao. Organotemplate-free and fast route for synthesizing beta zeolite. *Chemistry of materials*. 2008;20 (14):4533-5. <https://doi.org/10.1021/cm801167e>
- [29] Kamimura Y, Itabashi K, Okubo T. Seed-assisted, OSDA-free synthesis of MTW-type zeolite and "Green MTW" from sodium aluminosilicate gel systems. *Microporous and Mesoporous Materials*. 2012;147(1):149-56. <https://doi.org/10.1016/j.micromeso.2011.05.038>
- [30] Y. Kamimura KI, S.P. Elangovan, K. Itabashi, A. Shimojima, T. Okubo. OSDA-free synthesis of MTW-type zeolite from sodium aluminosilicate gels with zeolite beta seeds. *Microporous and Mesoporous Materials*. 2012;163:282-90. <https://doi.org/10.1016/j.micromeso.2012.07.014>
- [31] Luan H, Lei C, Ma Y, Wu Q, Zhu L, Xu H, et al. Alcohol-assisted synthesis of high-silica zeolites in the absence of organic structure-directing agents. *Chinese Journal of Catalysis*. 2021;42(4):563-70. [https://doi.org/10.1016/S1872-2067\(20\)63677-4](https://doi.org/10.1016/S1872-2067(20)63677-4)
- [32] Treacy M, Higgins J. *Collection of Simulated XRD Powder Patterns for Zeolites Fifth (5th) Revised Edition*. 2007.
- [33] Jacobs PA, Beyer HK, Valyon J. Properties of the end members in the Pentasil-family of zeolites: characterization as adsorbents. *Zeolites*. 1981;1(3):161-8. [https://doi.org/10.1016/S0144-2449\(81\)80006-1](https://doi.org/10.1016/S0144-2449(81)80006-1)
- [34] Wan Z, Wu W, Li G, Wang C, Yang H, Zhang D. Effect of SiO₂/Al₂O₃ ratio on the performance of nanocrystal ZSM-5 zeolite catalysts in methanol to gasoline conversion. *Applied Catalysis A: General*. 2016;523:312-20. <https://doi.org/10.1016/j.apcata.2016.05.032>
- [35] Shao J, Fu T-j, Chang J-w, Wan W-l, Qi R-y, Li Z. Effect of ZSM-5 crystal size on its catalytic properties for conversion of methanol to gasoline. *Journal of Fuel Chemistry and Technology*. 2017;45(1):75-83. [https://doi.org/10.1016/S1872-5813\(17\)30009-9](https://doi.org/10.1016/S1872-5813(17)30009-9)
- [36] Katada N, Igi H, Kim J-H. Determination of the Acidic Properties of Zeolite by Theoretical Analysis of Temperature-Programmed Desorption of Ammonia Based on Adsorption Equilibrium. *The Journal of Physical Chemistry B*. 1997;101(31):5969-77. <https://doi.org/10.1021/jp9639152>
- [37] Hu H, Lyu J, Rui J, Cen J, Zhang Q, Wang Q, et al. The effect of Si/Al ratio on the catalytic performance of hierarchical porous ZSM-5 for catalyzing benzene alkylation with methanol. *Catalysis Science & Technology*. 2016;6(8):2647-52. <https://doi.org/10.1039/C5CY01976A>
- [38] Thommes M. Physical adsorption characterization of nanoporous materials. *Chemie-Ingenieur-Technik*. 2010;82(7):1059-73. <https://doi.org/10.1002/cite.201000064>
- [39] Zaidi HA, Pant KK. Catalytic conversion of methanol to gasoline range hydrocarbons. *Catalysis Today*. 2004;96(3):155-60. <https://doi.org/10.1016/j.cattod.2004.06.123>
- [40] Saxena SK, Viswanadham N, Al-Muhtaseb AaH. Enhanced production of high octane gasoline blending stock from methanol with improved catalyst life on nano-crystalline ZSM-5 catalyst. *Journal of Industrial and Engineering Chemistry*. 2014;20(5):2876-82. <https://doi.org/10.1016/j.jiec.2013.11.021>
- [41] Zhao J, Wang Y, Sun C, Zhao A, Wang C, Zhang X, et al. Synthesis of hierarchical ZSM-5 aggregates by an alkali-treated seeds method with cetyltrimethylammonium bromide for the methanol to gasoline reaction. *Reaction Kinetics, Mechanisms and Catalysis*. 2019;128(2):1079-96. <https://doi.org/10.1007/s11144-019-01671-0>
- [42] Wan Z, Wu W, Chen W, Yang H, Zhang D. Direct Synthesis of Hierarchical ZSM-5 Zeolite and Its Performance in Catalyzing Methanol to Gasoline Conversion. *Industrial & Engineering Chemistry Research*. 2014;53(50):19471-8. <https://doi.org/10.1021/ie5036308>
- [43] Ghanbari B, Zangeneh FK, Rizzi ZT, Aghaei E. Highly Efficient Production of Benzene-Free Aromatics from Methanol over Low-Si/Al-Ratio Alkali-Modified Fe/Zn/HZSM-5. *ACS Omega*. 2018;3(12):18821-35.



- <https://doi.org/10.1021/acsomega.8b01380>
- [44] Qiao J, Wang J, Frenkel AI, Teng J, Chen X, Xiao J, et al. Methanol to aromatics: isolated zinc phosphate groups on HZSM-5 zeolite enhance BTX selectivity and catalytic stability. *RSC advances*. 2020;10(10):5961-71. <https://doi.org/10.1039/C9RA09657D>

